



OPEN ACCESS

EDITED BY
Wen Chen,
Yunnan University, China

REVIEWED BY
Peng Hu,
Chinese Academy of Sciences (CAS),
China
Xiangzhou Song,
Hohai University, China

*CORRESPONDENCE
Chunlei Liu,
✉ liuclei@gdou.edu.cn
Jiayi Cai,
✉ caijx2004y@nuist.edu.cn
Ning Cao,
✉ ncao@gdou.edu.cn

RECEIVED 01 July 2023
ACCEPTED 01 September 2023
PUBLISHED 20 September 2023

CITATION
Yang K, Liu C, Cai J, Cao N, Liao X, Su Q,
Jin L, Zheng R, Zhang Q and Wang L
(2023), The north–south shift of the ridge
location of the western Pacific
subtropical high and its influence on the
July precipitation in the Jianghuai region
from 1978 to 2021.
Front. Earth Sci. 11:1251294.
doi: 10.3389/feart.2023.1251294

COPYRIGHT
© 2023 Yang, Liu, Cai, Cao, Liao, Su, Jin,
Zheng, Zhang and Wang. This is an open-
access article distributed under the terms
of the [Creative Commons Attribution
License \(CC BY\)](https://creativecommons.org/licenses/by/4.0/). The use, distribution or
reproduction in other forums is
permitted, provided the original author(s)
and the copyright owner(s) are credited
and that the original publication in this
journal is cited, in accordance with
accepted academic practice. No use,
distribution or reproduction is permitted
which does not comply with these terms.

The north–south shift of the ridge location of the western Pacific subtropical high and its influence on the July precipitation in the Jianghuai region from 1978 to 2021

Ke Yang^{1,2,3,4}, Chunlei Liu^{1,2*}, Jiayi Cai^{4*}, Ning Cao^{1,2,3*},
Xiaoqing Liao^{1,2,3}, Qianye Su^{1,2,3}, Liang Jin^{1,2,3}, Rong Zheng^{1,2,3},
Qingkui Zhang⁵ and Lu Wang⁵

¹South China Sea Institute of Marine Meteorology, Guangdong Ocean University, Zhanjiang, China, ²CMA-GDOU Joint Laboratory for Marine Meteorology, Guangdong Ocean University, Zhanjiang, China, ³College of Ocean and Meteorology, Guangdong Ocean University, Zhanjiang, China, ⁴Nanjing University of Information Science and Technology, Nanjing, China, ⁵Fuyang Meteorology Bureau, Anhui, China

The Jianghuai region is the area between the Yangtze River and the Huai River in China and is a densely populated agriculture region therefore, the economics and human activity there are significantly affected by the precipitation changes, particularly during the summer when extreme storms and droughts normally occur. It will be helpful if the summer precipitation changes can be predicted. The monthly ERA5 atmospheric reanalysis data from 1978 to 2021 are used in this study to investigate the relationship between the ridge latitudinal location of the western Pacific subtropical high (WPSH) and the precipitation in July over the Jianghuai region. The results show that the WPSH ridge location has an important impact on the amount and spatial distribution of the precipitation in this region. When the ridge was northward, an anomalous anticyclonic circulation will appear over the western Pacific, leading to the weakening of the summer monsoon and the reduction of moisture transport from the Indian Ocean, therefore decreasing precipitation in the Jianghuai region, while the situation is opposite when the ridge was southward. The Niño 3.4 index in March and the India–Burma trough intensity index in June have significant correlations with the July WPSH ridge location, and both can be used as precursors to predict the WPSH ridge location and, therefore, the precipitation in this region.

KEYWORDS

western Pacific subtropical high, ridge location, Jianghuai region, precipitation, Niño 3.4, India–Burma trough intensity

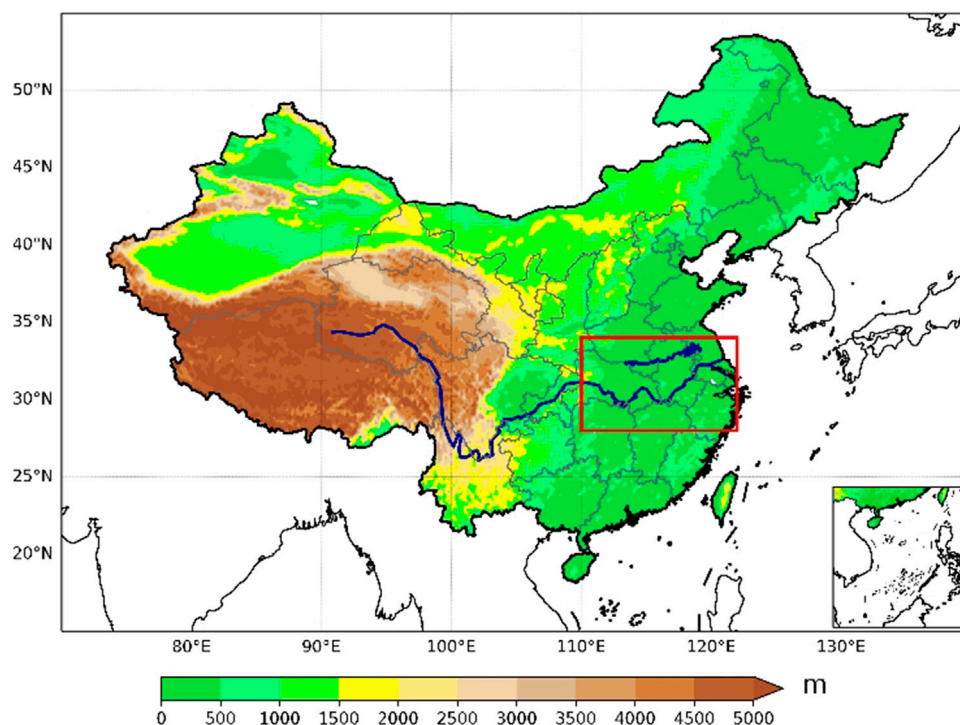


FIGURE 1

Topographic map of the land. The red rectangle shows the Jianghuai region (28–34°N, 110–122°E). The Yangtze River (long blue line in the south) and Huai River (short blue line in the north) are also displayed.

1 Introduction

The Jianghuai region shown in Figure 1 is between the Yangtze River and the Huai River and is mainly formed by the alluvial deposits of these two rivers, with low elevation generally less than 10 m. It is located in the transition belt from a subtropical to temperate zone, and the precipitation is affected by the East Asian monsoon, particularly by the Meiyu lasting normally from June to July. The land in the Jianghuai region is fertile for agriculture and is a famous area for fish and rice; it is one of the main granaries in China. However, this area is also prone to be affected by flood and drought (Yang et al., 2012; Wang et al., 2022). The precipitation amount and location over this region are often controlled by the western Pacific subtropical high (WPSH) through the steering flow around the WPSH (Huang et al., 2018).

The WPSH is a large-scale circulation system located in the troposphere over the western Pacific all year around and is one of the main parts of the East Asian summer monsoon (EASM) system, which has an important impact on the summer precipitation over eastern China (Yang and Sun, 2003; Tao et al., 2006; Jiang et al., 2011). The WPSH moves between 10 and 40°N, its longitudinal range is approximately 110–150°E, and it has significant seasonal variations.

The WPSH center is weak and gradually moves westward toward the mainland in spring from the ocean, and the WPSH strengthens and the center moves close to the East Asian continent in summer, with a northward shift of the WPSH ridge and the rain belt. The north–south shift of the WPSH ridge location controls the

movement of the rain belt in eastern Asia (Ren et al., 2005; Tao and Wei, 2006; Liu et al., 2013; Wu and Guo, 2019; Sun et al., 2022). For example, the summer precipitation in eastern China is mainly driven by the EASM and shows a zonal distribution (Zhou and R, 2005; Zhu et al., 2011), but the strength of the EASM is mainly affected by the WPSH (Huang and Sun, 1992; Lin and Wang, 2016).

Previous studies have shown that the meridional movement and anomalous activities of the WPSH are closely related to the distribution of the East Asian rain belt (Zhang et al., 2017). Yang et al. (2017) indicated that if the summer WPSH is located to the east, the summer precipitation in the Yellow River and Yangtze River basins will be relatively less, and *vice versa*. The cold and warm events in the equatorial central Pacific became the main forcing in the late 1990s, and the impact of the WPSH on the EASM precipitation has weakened (Huang et al., 2018). It was also found by He et al. (2001) that the coastal sea surface temperature (SST) has a significant impact on the interannual anomaly of the WPSH, and the sensible heat caused by the SST may stimulate the anomalous anticyclonic circulation on the west side of the WPSH and then affect the intensity and latitudinal location of the WPSH.

The forcing of different SST anomaly distributions on atmospheric dynamic processes is one of the important reasons for the interannual variation of the WPSH location. During the El Niño mode with positive SST anomalies in the central and eastern Pacific, the wave–wave and wave–current interactions in the atmosphere are weak, leading to the southward shift of the WPSH ridge. However, when the atmospheric circulation is forced by the central Pacific La Niña mode, the wave–wave and

wave–current interactions are stronger, making the WPSH ridge shift northward (Cao et al., 2009). Wen et al. (2003) pointed out that the diabatic heating in the north side of the WPSH can obstruct its northward movement in summer. The diabatic heating includes the sensible heating associated with the SST. However, the study by Ai et al. (2000) showed that the SST in the western Pacific only has weak correlation with the WPSH location.

Studies have shown that since the 1980s, climate warming has led to more frequent occurrences of extreme floods and droughts in the Jianghuai region, usually in consecutive seasons or years, with floods and droughts occurring alternately in July (Qian et al., 2007). Yang Y. et al. (2022) pointed out that under the effect of greenhouse warming, the response of the tropical atmospheric convection to the SST anomaly increases, so does the response of the WPSH circulation, leading to an increase in the frequency of strong WPSH events which are defined as the cases of PC1 > 1.5 STD (standard deviation of PC1), where PC1 is the first principal component of the empirical orthogonal function (EOF) calculated from the averaged JJA (June, July, and August) 850-hPa streamfunction anomalies. On the other hand, He et al. (2015) pointed out that under the climate warming, the WPSH showed a strong signal of weakening and eastward retreat in the middle troposphere, and they indicated that the meridional temperature gradient is the main factor affecting the WPSH in the middle troposphere.

The north–south shift of the WPSH location plays a decisive role in summer precipitation in East Asia and has attracted a lot of attention in many recent studies (Zhang et al., 2022), but the factors affecting the anomaly of the north–south location of the WPSH ridge have not yet been fully understood, leading to errors in the prediction of ridge positions. For the precipitation in the Jianghuai region, the following questions can be asked: 1) How is the WPSH ridge location related to the summer precipitation in the Jianghuai region? 2) Can the ridge location be predicted, and what factors affect the location? 3) Has the climate warming changed the relationship between the WPSH ridge location and the precipitation in the Jianghuai region in recent years? The purpose of this study is to explore the relationship between the precipitation in the Jianghuai region and the WPSH ridge location and to understand the characteristics of the anomalous activities of the WPSH ridge. The factors affecting the WPSH ridge movement are also investigated.

2 Data and methods

The monthly mean ERA5 (the fifth generation ECMWF ReAnalysis) data (Hersbach et al., 2020) over 1978–2021 have been employed in this study, including the geopotential height, wind speed, specific humidity, relative vorticity, outgoing longwave radiation (OLR), and precipitation, with the horizontal resolution of $0.25^\circ \times 0.25^\circ$. The 5880 gpm isolines at 500 hPa describe the WPSH characteristics and are also used to stand for the main body of the WPSH. The climatology is the mean from 1978 to 2021. The observed precipitation over land from the Global Precipitation Climatology Centre (GPCC, Rudolf et al., 2010) is also used for comparison.

The WPSH ridge location is defined as the separation latitude between the easterly and westerly within the range of (10–60°N, 110–150°E) at 500 hPa. The WPSH center at each longitude is estimated using the condition of $u = 0$ and $\partial u / \partial y > 0$, where u is the zonal component of the wind and y is the meridional direction, and then, the mean WPSH ridge latitude is estimated by averaging these WPSH center locations. The difference between the grid point geopotential height at 500 hPa in the region (15–20°N, 80–100°E) and 5800 gpm is multiplied by the grid area, and the summation of the difference is defined as the India–Burma trough intensity index. The monthly mean Niño 3.4 index is calculated from the area mean ERA5 SST anomaly (SSTA) averaged over (5°S–5°N, 120–170°W) and is used to study the relationship between the SST and the WPSH ridge location. The range of the Jianghuai area is (28–34°N, 110–122°E). Unless otherwise stated, the anomalies are computed relative to the reference period 1978–2021.

The East Asia–Pacific (EAP) teleconnection index is also used here to study the influences of the large-scale circulation on the movement of the WPSH ridge. The EAP was first proposed by Huang and Li (1987) and Nitta (1987); when the temperature of the western Pacific warm pool is low, weakened convective activity occurs over the Philippines and the Maritime Continent, leading to a “+ – +” EAP teleconnection pattern, with more precipitation in the Yangtze–Huai River Basin, Korean Peninsula, and Japan area, and *vice versa*. Based on the work of Huang (2004), the EAP index is defined as follows:

$$\text{EAP} = \text{Nor}(-0.25Z'_{S1} + 0.5Z'_{S2} - 0.25Z'_{S3}), \quad (1)$$

where $Z' = Z - \bar{Z}$, Z is the geopotential height at 500 hPa, \bar{Z} is the climatology over 1978–2021, $Z'_S = Z' \sin 45^\circ / \sin \varphi$, φ is the latitude, and $\text{Nor}(X)$ is the standardization of X . Z'_{S1} is calculated at (20°N, 125°E), Z'_{S2} at (40°N, 125°E), and Z'_{S3} at (60°N, 125°E). The t -test is used to evaluate the statistical significance and the correlation between variables is calculated using the Pearson correlation. The significant correlation means it passed the test using Pearson critical values at the 95% significance level.

3 Results

3.1 Relationship between the WPSH ridge location and precipitation in July over the Jianghuai region

The seasonal variations of the area mean precipitation in the Jianghuai region are plotted in Figure 2A. It shows that the July precipitation amount is the second largest after June; it can cause floods due to the accumulation of the precipitation from June to July (Qian et al., 2007). The north–south shift of the July ridge is also larger than the June one (Figure 2B). By analyzing the daily precipitation in June and July (not shown here), it is found that the high precipitation is concentrated from late June to early July, and the July WPSH ridge location has significant correlation (−0.45) at 95% significance level with July precipitation over the Jianghuai region, but the June ridge only has small correlation (<|0.2|) with June precipitation over this area. Therefore, the relationship between

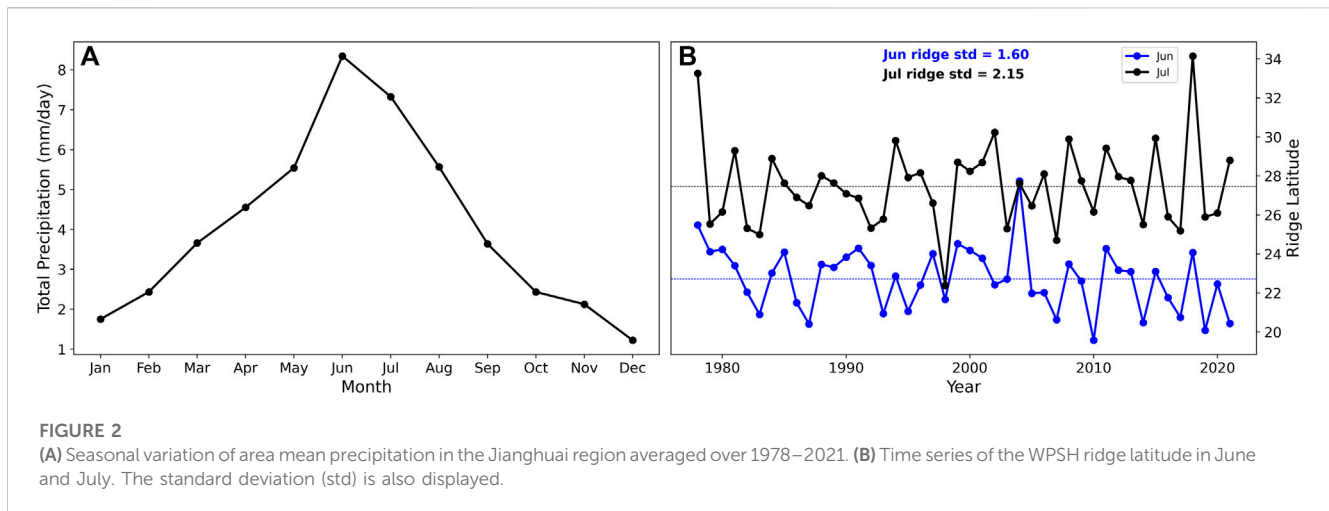


FIGURE 2
(A) Seasonal variation of area mean precipitation in the Jianghuai region averaged over 1978–2021. (B) Time series of the WPSH ridge latitude in June and July. The standard deviation (std) is also displayed.

the July ridge location and July precipitation in the Jianghuai region will be analyzed in this study.

The time series of the area mean precipitation in the Jianghuai region and the WPSH ridge latitude in July are plotted in Figure 3A, and they are significantly negatively correlated (Figure 3B), with the correlation coefficient $r = -0.48$ over 1978–2021. That is, the total July precipitation in the Jianghuai region decreases in years when the WPSH ridge is further northward and increases when the WPSH ridge is further southward. The correlation coefficient is $r = -0.59$ (Figure 3C) over 1978–1997 and $r = -0.43$ over 1998–2021 (Figure 3D). The weakening relationship in the last 2 decades may be because the central El Niño phenomenon became the dominant mode in the Pacific after late 1990s, which caused the Indo-Pacific Walker circulation to move significantly westward, leading to the weakening of the relationship between the WPSH and the East Asian summer monsoon (Huang and Sun, 1992).

To further study the influence of the ridge location on the precipitation in the Jianghuai region, the WPSH ridge locations from 1978 to 2021 are sorted in the ascending order, and the top 6 years are defined as the northward years (1978, 1994, 2002, 2008, 2015, and 2018), the bottom six are defined as southward years (1982, 1983, 1998, 2003, 2007, and 2017), and the rest years are normal years. Figure 4 shows the spatial distribution of the composite July precipitation anomalies calculated from ERA5 and GPCC in the Jianghuai region (red box) during the northward (Figures 4A, C) and southward (Figures 4B, D) years. When the WPSH ridge is northward (Figure 4A), the precipitation anomaly from ERA5 data shows significantly more precipitation in the Jianghuai region (south of 28°N) and less precipitation north of 28°N. The positive extreme precipitation anomaly is located in the southwest to the Jianghuai region, and the negative extreme value center is located in the northeast and west of the Jianghuai region. However, the precipitation anomaly shows opposite south–north distribution in southward years (Figure 4B), and the northwestern part of the Jianghuai region has more precipitation, and the southeastern part has less precipitation. Therefore, the meridional shift of the WPSH ridge location in July affects the precipitation amount and the spatial distribution in the Jianghuai area. This is also checked using the GPCC data which are based on observations, and the results in Figures 4C, D show similar patterns.

The differences in precipitation spatial distribution shown in Figure 4 can be further investigated by looking into the moisture transport in this region. Comparing the moisture transport in northward years (Figure 5A) and southward years (Figure 5B), it can be seen that the moisture originated from the Indian Ocean passes through the South China Sea and reaches the Jianghuai region from the south in northward years, and a fraction of the moisture is transported northeastward through the South China Sea to the western Pacific (Figure 5A). In southward years, the moisture comes from both the Indian Ocean and the western Pacific, and both merge in the south of Taiwan island under the influences of the WPSH steering flow and arrive at the Jianghuai region.

The anomalies in moisture transport (Figure 5C) show a cyclonic circulation over the western Pacific and the northeasterly wind over the Jianghuai region in northward years, leading to the weakening of the EASM and suppressing the moisture transport from the Indian Ocean. Meanwhile, the easterly wind in the southern part of the WPSH weakened, causing the directly northward moisture transport from the southern part of the Japanese island, but the moisture does not reach the Jianghuai region. Under the combined influences of the weak summer monsoon and the weak easterly wind south of the WPSH, there is less moisture transported to the Jianghuai region than in normal years, resulting in a decrease in precipitation in the region (Figure 5C). On the contrary, the anomalous anticyclonic circulation in the western Pacific in southward years makes the EASM stronger and the enhanced southwesterly wind in the Jianghuai region. The easterly wind in the south of the WPSH was strengthened at the same time, and the Pacific moisture was transported northward along the periphery of the WPSH in the south of Taiwan island to the Jianghuai region. The strengthening of the summer monsoon and the southeasterly wind of the WPSH leads to more moisture transport from the Indian Ocean and the western Pacific to the Jianghuai region, resulting in the precipitation increase there (Figure 5D). The corresponding horizontal moisture divergence in northward years (Figure 5E) shows similar patterns to the precipitation distribution in Figures 4A, C. The northern part of the Jianghuai region is an anomalous moisture divergence area, and the southern part has the anomalous moisture convergence. The situation is reversed in southward years (Figure 5F).

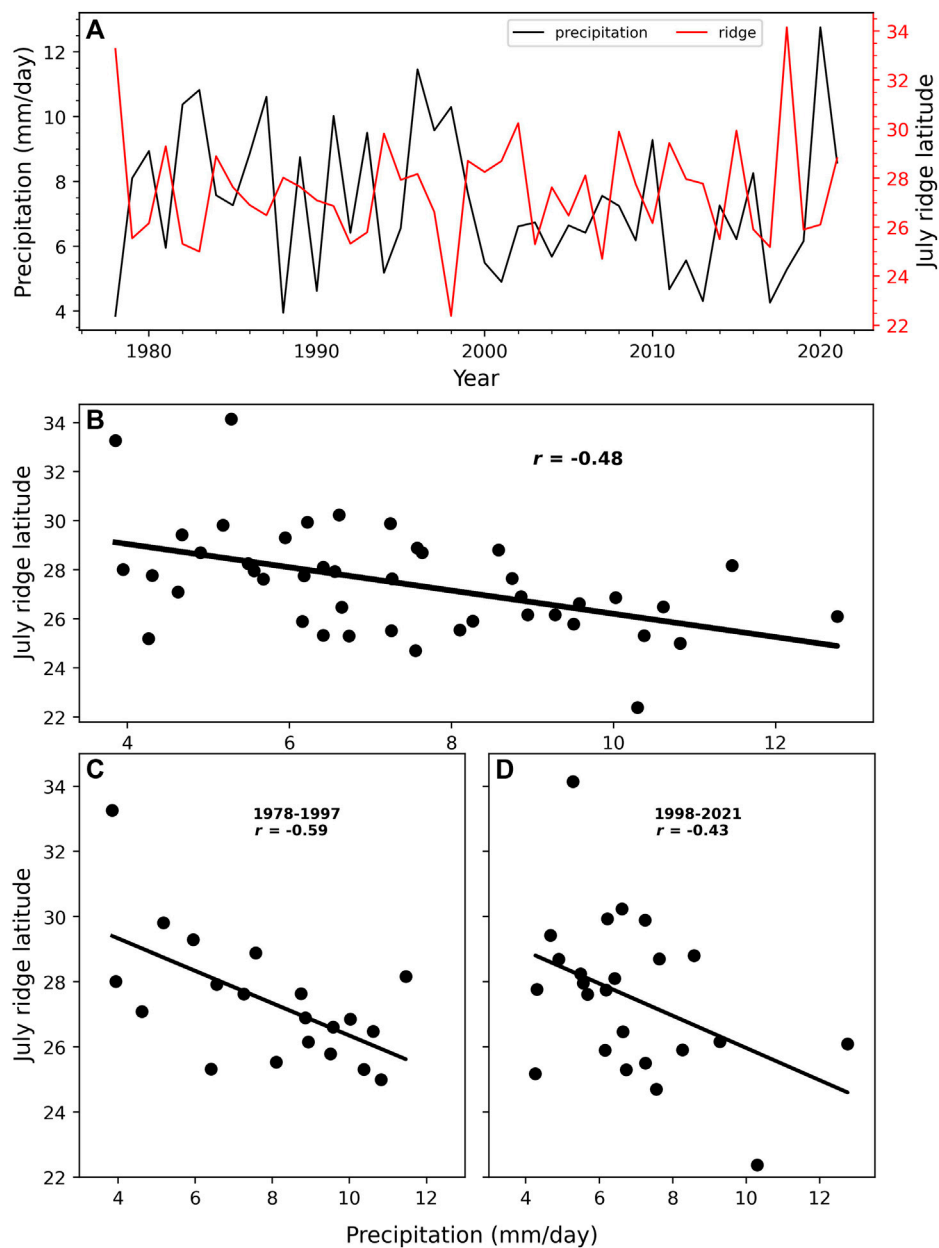
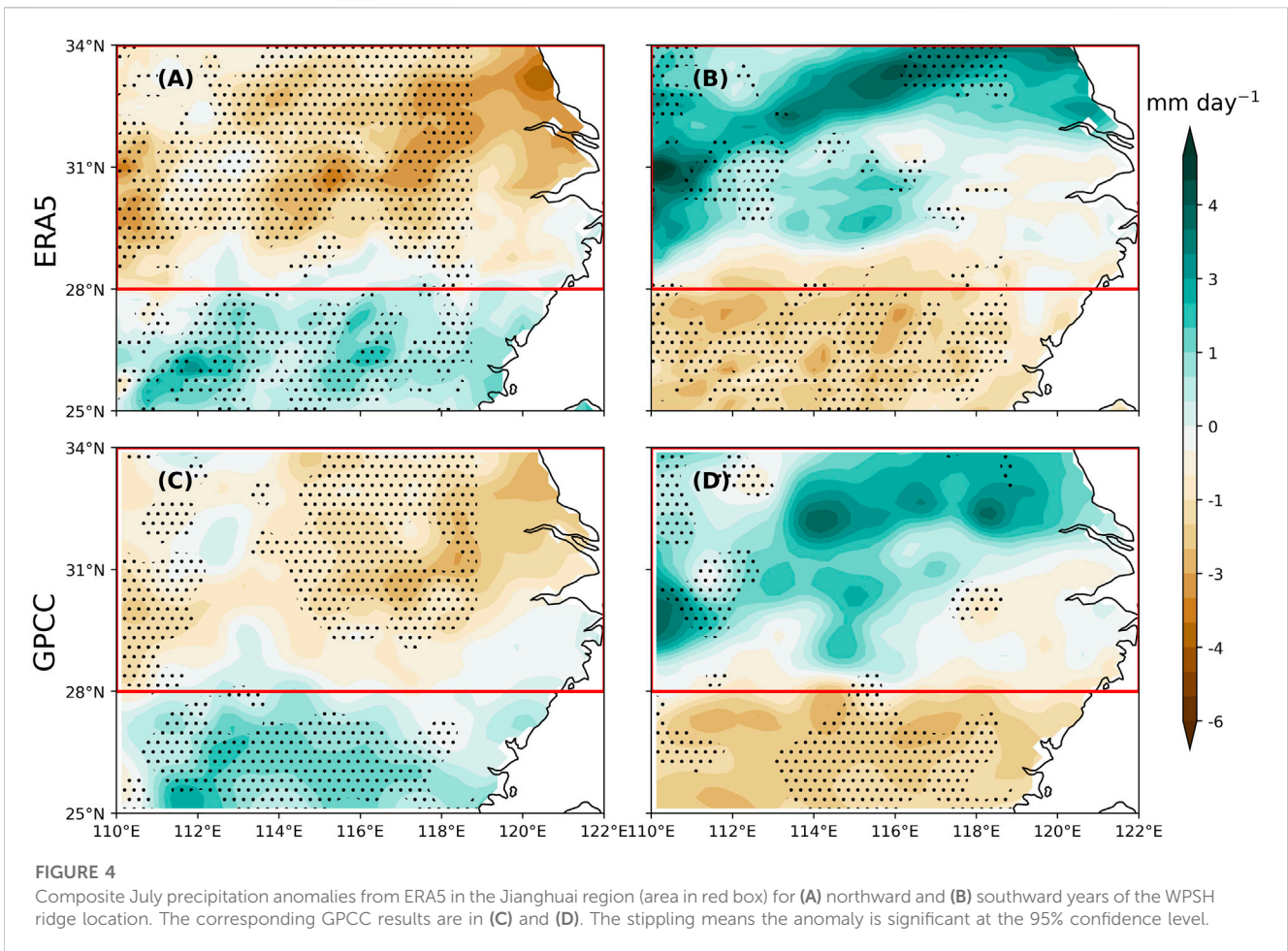


FIGURE 3 (A) The time series of the area mean precipitation in Jianghuai region and the WPSH ridge latitude in July. The scatter plot between the area mean precipitation and the WPSH ridge latitude over (B) 1978–2021, (C) 1978–1997, and (D) 1998–2021.

3.2 Changes in environmental conditions related to the WPSH ridge shift

Considering the close relationship between the local and large-scale circulations (Ding, 1992; Fukutomi and Yasunari, 1999), and for further understanding the WPSH ridge shift, the characteristics of the geopotential height at 500 hPa in northward and southward years are analyzed. The geopotential height anomalies in northward years show a zonal distribution in middle and high latitudes and a ‘- + -’ meridional distribution pattern in East Asia from low to high latitudes, consistent with the positive EAP teleconnection pattern.

Both the Ural Mountains and the Yakutsk region are in the negative anomaly region, indicating that the high-pressure ridge over the Ural Mountains and the Yakutsk region has not yet been established, and the blocking has not been formed. The main body of the WPSH is located over the ocean, its area is smaller, and its location is further northeast compared with the climatology (Figure 6A). The anomalous circulation in Figure 6B shows a ‘+ - +’ distribution from low to high latitudes in East Asia, consistent with the negative EAP teleconnection pattern. There is a positive anomaly over the Ural Mountains and a weak positive anomaly over the Yakutsk, indicating the establishment of the high pressure ridge over the Ural



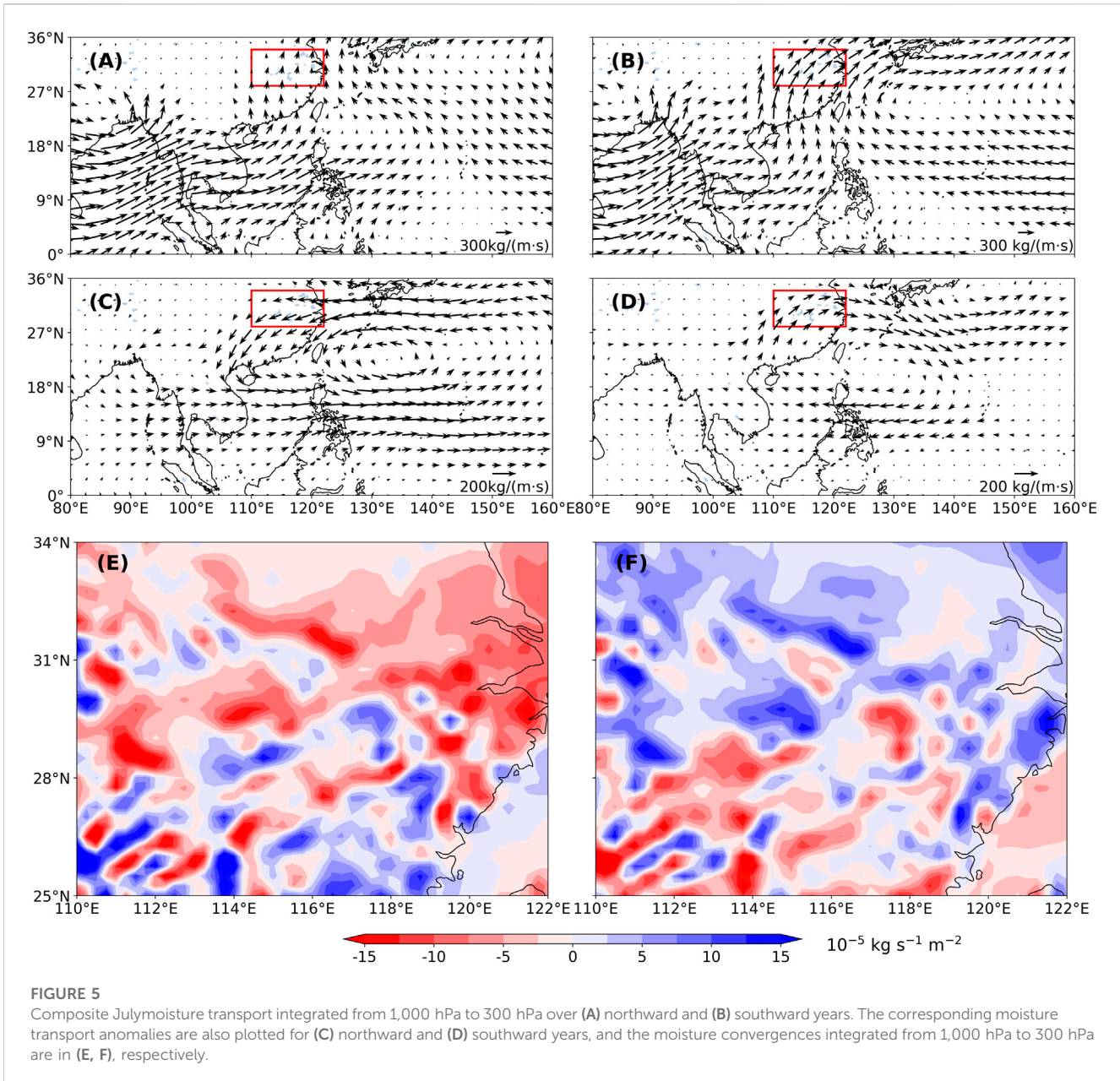
Mountains and the Yakutsk, and the blocking has been gradually formed at high latitudes. Meanwhile, a westerly flow appears in the mid-latitudes, and there is a negative anomaly near Lake Baikal and a low pressure begins to establish. The main body of the WPSH is close to the continent, its area is larger, and its location is further southwest compared with the climatology (Figure 6B), and the moisture can be transported to the Jianghuai region by the southeasterly steering flow of the WPSH (Figure 5B).

It can be seen from Figure 6A that the westerly belt at middle and high latitudes and the significant positive anomaly near Japan island lead to anomalous anticyclonic circulation, which will promote the northward movement of the WPSH ridge. In Figure 6B, there is a blocking situation at high latitudes at 500 hPa, and the significant anomalous cyclonic circulation near Japan island will inhibit the northward movement of the WPSH and cause the southward WPSH ridge location. The EAP is closely related to the summer precipitation in China and the precipitation from East Asia to the western Pacific (Yu et al., 2009). The correlation coefficient $r=0.65$ between the EAP index and the WPSH ridge locations over 1978–2021 is significant in this study, implying that when the EAP index is high, the WPSH ridge latitude will be further north, and *vice versa*.

The OLR represents the convection strength, and the composite July OLR anomalies in northward and southward years are plotted in Figure 7. The OLR anomaly in northward years shows a “+ - +”

distribution from low to high latitudes over East Asia, and there is a significant negative OLR anomaly region from the Philippines to the western Pacific where the convective activities are significantly strengthened. Meanwhile, there is a significant positive OLR anomaly near Japan island, and the convective activity is significantly weakened compared with normal years. However, the distribution of the OLR anomaly in southward years over East Asia is almost opposite to that in northward years. The area from the Philippines to the western Pacific has a significant positive anomaly, and the convective activity is weaker than that in normal years. There is a significant negative OLR anomaly in the area from the Yangtze River Basin to Japan island, and the convective activity is significantly stronger than normal (Figure 7B), consistent with the precipitation distribution shown in Figures 4B, D. Therefore, when the OLR in the western Pacific is anomalously negative (positive), the convective activity will be enhanced (weakened), which will trigger a positive (negative) EAP-type teleconnection (Gong et al., 2018), corresponding to the northward (southward) WPSH ridge location.

The latitude–height cross sections of the composite relative vorticity anomaly averaged over the WPSH region (110°E–150°E) are plotted in Figure 8. In northward years, the relative vorticity anomalies from 1,000 hPa to 200 hPa all show the “- + - +” distribution from the low to high latitudes, and the maximum and minimum centers are concentrated in the lower layer from 1,000 hPa to 850 hPa. The minimum is located near 40°N, and the



maximum is located near 30°N (Figure 8A). There is an anomalous cyclonic circulation at 500 hPa from 20 to 30°N and an anomalous anticyclonic circulation from 30 to 40°N. The anomalous anticyclonic vorticity north of the WPSH strengthens the westerly wind in the northern part of the WPSH, and the convergent airflow leads to a pressure increase. While the anomalous cyclonic vorticity south of the WPSH weakens the easterly and the divergent airflow leads to a pressure decrease, which is conducive to the northward movement of the WPSH ridge. The composite relative vorticity anomaly distribution pattern in southward years is almost opposite to that in northward years. The vorticity anomaly from the low to high latitudes shows ‘+ - -’ distribution, the minimum is located near 28°N, and the maximum is located near 40°N (Figure 8B). There is an anomalous anticyclonic circulation at 500 hPa from 20 to 30°N,

and an anomalous cyclonic circulation from 30 to 40°N. The anomalous cyclonic vorticity north of the WPSH and the anomalous anticyclonic vorticity south of the WPSH result in the divergence of airflow on the north side of the WPSH and the convergence of airflow on the south side, reducing the air pressure on the north side of the WPSH and increasing the pressure on the south side, thereby inhibiting the northward movement of the WPSH (Wen et al., 2003).

3.3 Precursors affecting the WPSH ridge location

The aforementioned results have shown the important influences of the WPSH ridge movement on the precipitation

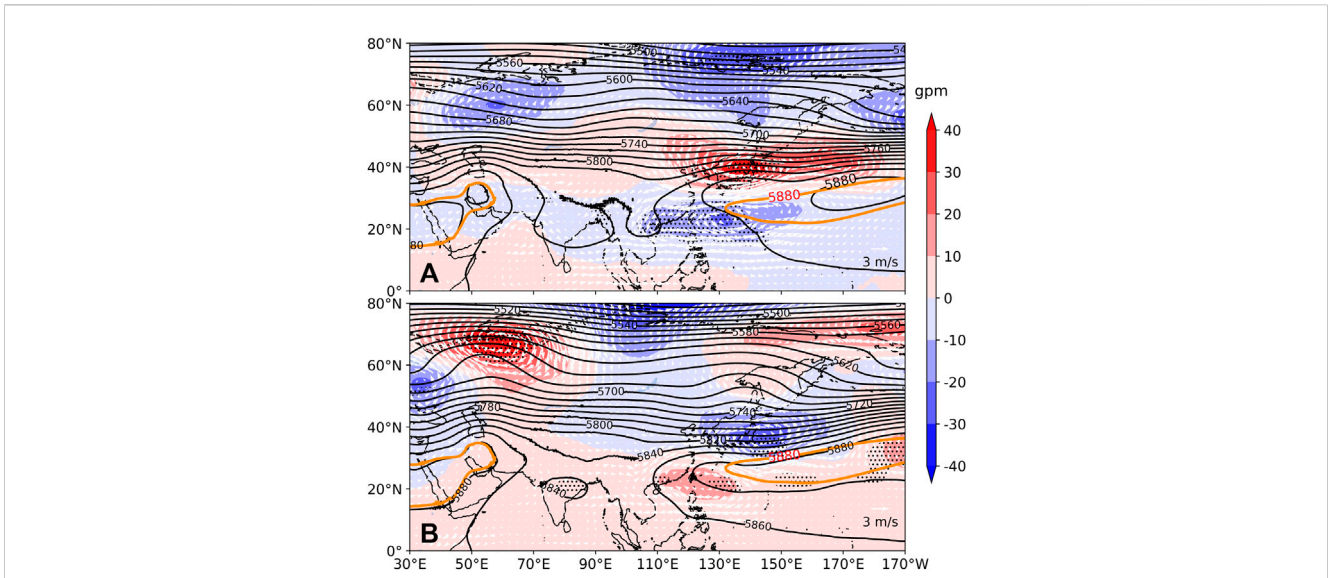


FIGURE 6 Composite geopotential height (contours) and anomalies (shadings) at 500 hPa in (A) northward and (B) southward years. The wind anomaly (white arrow) is also displayed. The stippling means the anomaly is significant at the 95% confidence level. The solid orange line is the climatology of 5,880 gpm contour.

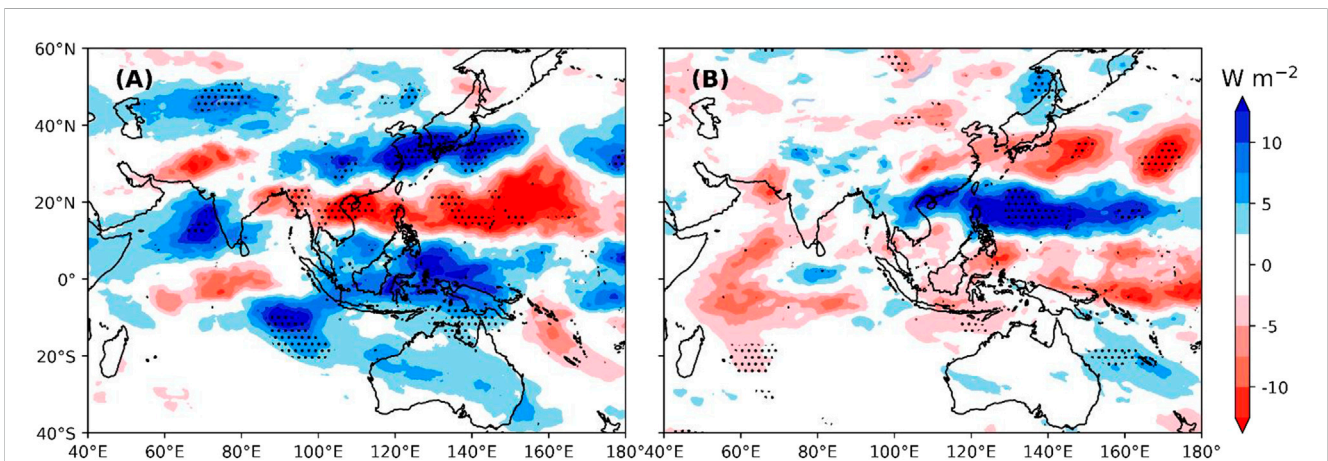
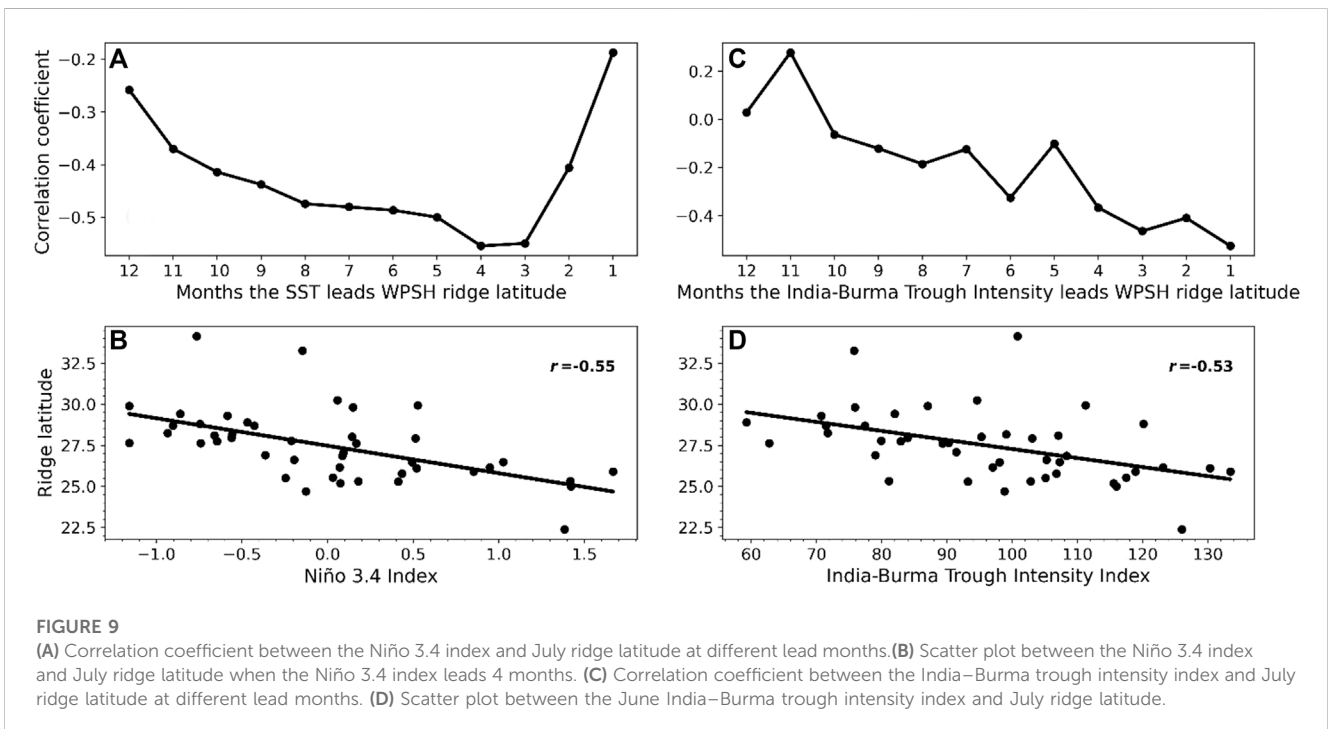
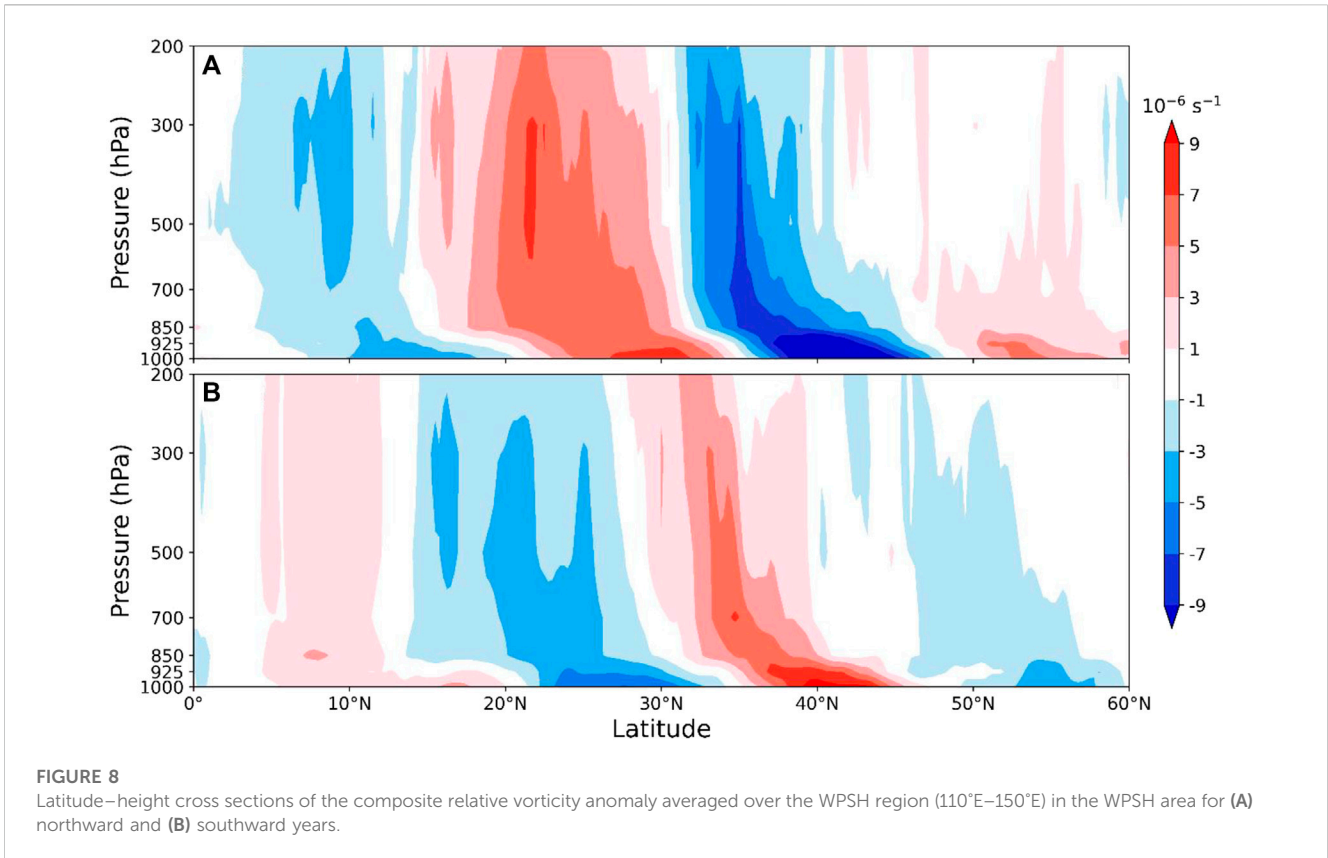


FIGURE 7 Composite July OLR anomalies in (A) northward and (B) southward years. The stippling means the anomaly is significant at the 95% confidence level.

in July over the Jianghuai region, it will be helpful if the ridge shift can be predicted using some precursors. Although the July WPSH ridge latitude and the July EAP index have a significant positive correlation, the lead correlation from the EAP index is not high enough for the prediction. Previous studies have shown that the SST has significant influences on the atmosphere, and it can be a lead precursor sometimes (Lau, 1997; Czaja and Frankignoul, 1999; Wu and Chen, 2020). The correlation between the SST anomaly in the Niño 3.4 region and the WPSH ridge location has been plotted in Figure 9A. The absolute value of the correlation coefficient reaches the maxima when the SSTA leads 4 months with $r = -0.55$, that is, the SSTA time series in March can be used to predict the ridge location to

some degrees. The scatter plot between the SSTA in March and the ridge location in July is shown in Figure 9B.

The tropospheric westerly is split into the southern branch and the northern branch by the blocking of the large terrain Qinghai–Tibet Plateau. The southern branch is a large-scale trough known as the India–Burma trough. There is a close interannual relationship between the India–Burma trough and the precipitation anomalies in Asia, and this relationship has shown a strengthening trend in recent decades (He et al., 2000; Wang et al., 2011). The India–Burma trough has long been considered as one of the important factors affecting the weather and climate in East Asia. The correlation coefficients between the India–Burma trough intensity index and the WPSH ridge latitude in July are plotted in Figure 9C. The correlation



reaches the significant minima of $r = -0.53$ when the India–Burma trough intensity index in June is used. Therefore, when the intensity of the India–Burma trough is strong in June, the WPSH ridge will be more southward in July, and *vice versa*.

4 Discussion and conclusion

The Jianghuai region is a densely populated area and one of the main granaries in China, but it is also prone to flood and drought,

particularly in July when the accumulated extreme precipitation can cause severe flood (Qian et al., 2007). Therefore, it will be helpful if the July precipitation can be predictable. The influence of the WPSH ridge location on the July precipitation in the Jianghuai region has been investigated in this study, and the precursors used to predict the WPSH ridge location have been revealed. The main conclusions are given as follows:

- 1) The WPSH ridge location has an important impact on the amount and spatial distribution of the precipitation in the Jianghuai region. When the ridge was northward in July, an anomalous anticyclonic circulation will appear in the western Pacific, leading to the weakening of the summer monsoon and the reduction of moisture transport from the Indian Ocean to the Jianghuai region. When the WPSH ridge is southward, an anomalous cyclonic circulation will appear in the western Pacific, causing the strengthening of the summer monsoon and the enhancement of the moisture transport from the Indian Ocean and western Pacific to the Jianghuai region, increasing the moisture amount. The divergence of the moisture in the south of the Jianghuai area and the convergence in the north result in less precipitation in the south of the Jianghuai area and more in the north.
- 2) The geopotential height at 500 hPa and OLR in northward and southward years of the WPSH ridge are closely associated with the EAP-type teleconnections. The correlation coefficient $r=0.65$ between the EAP index and the WPSH ridge location over 1978–2021 is significant, and it implies that when the EAP index is high, the WPSH ridge latitude will be further north, and *vice versa*. When the OLR in the western Pacific is anomalously negative (positive), the convective activity will be enhanced (weakened), which will trigger a positive (negative) EAP-type teleconnection (Gong et al., 2018), corresponding to the northward (southward) WPSH ridge location.
- 3) The WPSH ridge location is affected by the El Niño event. The Niño 3.4 index leads the ridge location 4 months, and the correlation coefficient can reach -0.55 ; therefore, the Niño 3.4 index in March can be used to predict the ridge location and the precipitation amount and spatial distribution in the Jianghuai region. The India–Burma trough intensity index in June also has a significant strong negative correlation with the WPSH ridge location in July, with the correlation coefficient $r=-0.53$. So, both the Niño 3.4 index and the India–Burma trough intensity index can be used as precursors to forecast the July WPSH ridge location and, therefore, precipitation in the Jianghuai region.

Only the relationship between the WPSH ridge location and the precipitation over the Jianghuai region in July has been investigated in this study. The moisture transport to the Jianghuai region (Yang K. et al., 2022), the extreme precipitation variation (Liu et al., 2012; Liu and Allan, 2013), and the decadal changes in the relationship between the WPSH ridge location and precipitation in the Jianghuai region have not been further investigated and will be conducted in a future study. The change in the relationship in other summertime months also needs full investigation in order to have a deep understanding of the variability in the summer precipitation over

the Jianghuai region. As the multiple linear regression (MLR) method has already been widely employed in other studies (Ai and Chen 20002; Li et al., 2023), it can also be used to predict the WPSH ridge location. The wavelet coherence and cross spectrum (Grinsted et al., 2004) have been reported to have better depiction of the changes in the interannual relationship. These methods can be used to check the robustness of this study in the future work.

Data availability statement

The original contributions presented in the study are included in the article/supplementary material; further inquiries can be directed to the corresponding authors.

Author contributions

All authors listed have made a substantial, direct, and intellectual contribution to the work and approved it for publication.

Funding

This work was jointly supported by the National Natural Science Foundation of China (42075036 and 42275017); the LASG key open project (20230273) from the Institute of Atmospheric Physics, Chinese Academy of Sciences; Fujian Key Laboratory of Severe Weather (2021KFKT02); the scientific research start-up grant of Guangdong Ocean University (R20001); and the Postgraduate Education Innovation Project of Guangdong Ocean University (202144 and 202253).

Acknowledgments

The authors thank two reviewers for reviewing this paper and providing constructive comments and suggestions.

Conflict of interest

The authors declare that the research was conducted in the absence of any commercial or financial relationships that could be construed as a potential conflict of interest.

Publisher's note

All claims expressed in this article are solely those of the authors and do not necessarily represent those of their affiliated organizations, or those of the publisher, the editors, and the reviewers. Any product that may be evaluated in this article, or claim that may be made by its manufacturer, is not guaranteed or endorsed by the publisher.

References

- Ai, Y., and Chen, X. (2000). Analysis of the correlation between the subtropical high over western Pacific in summer and SST. *J. J. Trop. Meteorology* 16, 1–8. doi:10.3969/j.issn.1004-4965.2000.01.001
- Cao, J., Yang, R., You, Y., and Huang, W. (2009). The mechanism for the impact of sea surface temperature anomaly on the ridgeline surface of Western Pacific. *Sci. China Ser. D-Earth Sci.* 52, 1864–1870. doi:10.1007/s11430-009-0149-1
- Czaja, A., and Frankignoul, C. (1999). Influence of the north atlantic SST on the atmospheric circulation. *Geophys. Res. Lett.* 26 (19), 2969–2972. doi:10.1029/1999gl900613
- Ding, Y. (1992). Summer monsoon rainfalls in China. *J. J. Meteorological Soc. Jpn. Ser. II.* 70, 373–396. doi:10.2151/jmsj1965.70.1b_373
- Fukutomi, Y., and Yasunari, T. (1999). 10–25 day intraseasonal variations of convection and circulation over East Asia and western North Pacific during early summer. *J. Meteorological Soc. Jpn. Ser. II.* 77, 753–769. doi:10.2151/jmsj1965.77.3_753
- Gong, Z., Feng, G., Dogar, M. M., and Huang, G. (2018). The possible physical mechanism for the EAP–SR co-action. *Clim. Dyn.* 51, 1499–1516. doi:10.1007/s00382-017-3967-4
- Grinsted, A., Moore, J. C., and Jevrejeva, S. (2004). Application of the cross wavelet transform and wavelet coherence to geophysical time series. *NonlinProcesses Geophys* 11, 561–566. doi:10.5194/npg-11-561-2004
- He, C., Zhou, T., Lin, A., Wu, B., Gu, D., Li, C., et al. (2015). Enhanced or weakened western North Pacific subtropical high under global warming? *Sci. Rep.* 5, 16771. doi:10.1038/srep16771
- He, J. H., Bing, Z., Min, W., and Feng, L. (2001). Vertical circulation structure, interannual variation features and variation mechanism of western pacific subtropical high. *Adv. Atmos. Sci.* 18, 497–510. doi:10.1007/s00376-001-0040-2
- He, J. (2000). Large-scale features of the onset of South China Sea summer monsoon and the physical mechanism (in Chinese). *Clim. Environ. Res.* 5, 333–344. doi:10.3969/j.issn.1006-9585.2000.04.001
- Hersbach, H., Bell, B., Berrisford, P., Hirahara, S., Horányi, A., Muñoz-Sabater, J., et al. (2020). The ERA5 global reanalysis. *Q. J. R. Meteorol. Soc.* 146, 1999–2049. doi:10.1002/qj.3803
- Huang, G. (2004). An index measuring the interannual variation of the East asian summer monsoon—the EAP index. *Adv. Atmos. Sci.* 21, 41–52. doi:10.1007/BF02915679
- Huang, R. H., and Li, W. J. (1987). “Influence of heat source anomaly over the tropical western Pacific on the subtropical high over East Asia,” in Proc. International Conference on the General Circulation of East Asia, Chengdu, China, April 10–15. 1987, 40–45.
- Huang, R. H., and Sun, F. Y. (1992). Impacts of the tropical western Pacific on the East Asian summer monsoon. *J. Meteor. Soc. Jpn.* 70, 243–256. doi:10.2151/jmsj1965.70.1b_243
- Huang, Y., Wang, B., Li, X., and Wang, H. (2018). Changes in the influence of the western Pacific subtropical high on Asian summer monsoon rainfall in the late 1990s. *Clim. Dyn.* 51, 443–455. doi:10.1007/s00382-017-3933-1
- Jiang, X., Li, Y., Yang, S., and Wu, R. (2011). Interannual and interdecadal variations of the South Asian and western Pacific subtropical highs and their relationships with Asian-Pacific summer climate. *Meteorology Atmos. Phys.* 113, 171–180. doi:10.1007/s00703-011-0146-8
- Lau, N. C. (1997). Interactions between global SST anomalies and the midlatitude atmospheric circulation. *Bull. Am. Meteorological Soc.* 78, 21–33. doi:10.1175/1520-0477(1997)078<0021:ibgsaa>2.0.co;2
- Li, Y., Wei, K., Chen, K., He, J., Zhao, Y., Yang, G., et al. (2023). Forecasting monthly water deficit based on multi-variable linear regression and random forest models. *Water* 15 (6), 1075. doi:10.3390/w15061075
- Lin, Z., and Wang, B. (2016). Northern East Asian low and its impact on the interannual variation of East Asian summer rainfall. *Clim. Dyn.* 46, 83–97. doi:10.1007/s00382-015-2570-9
- Liu, C., Allan, R. P., and Huffman, G. J. (2012). Co-variation of temperature and precipitation in CMIP5 models and satellite observations. *Geophys. Res. Lett.* 39, L13803. doi:10.1029/2012GL052093
- Liu, C., and Allan, R. P. (2013). Observed and simulated precipitation responses in wet and dry regions 1850–2100. *Environ. Res. Lett.* 8 (3), 034002. doi:10.1088/1748-9326/8/3/034002
- Liu, Y. M. (2013). Meiyu flooding of Huaihe River valley and anomaly of seasonal variation of subtropical anticyclone over the western Pacific. *Chin. J. Atmos. Sci.* 37, 439–450. doi:10.3878/j.issn.1006-9895.2012.12313
- Nitta, T. (1987). Convective activities in the tropical western Pacific and their impact on the Northern Hemisphere summer circulation. *J. Meteor. Soc. Jpn.* 64, 373–390. doi:10.2151/jmsj1965.65.3_373
- Qian, Y. F. (2007). Studies of floods and droughts in the yangtze-huaihe River basin. *Chin. J. Atmos. Sci.* 31, 1279–1289.
- Ren, H. (2005). Dynamical model of Subtropical High ridge-line section and numerical simulations with its simplified scheme. *Chin. J. Atmos. Sci.* 29, 71–78.
- Rudolf, B. (2010). *The new ‘GPCC Full Data Reanalysis version 5’ providing high-quality gridded monthly precipitation data for the global land-surface is public available since December 2010 GPCC Status Report.*
- Sun, C., Shi, X., Yan, H., Jiang, Q., and Zeng, Y. (2022). Forecasting the June ridge line of the western pacific subtropical high with a machine learning method. *Atmosphere* 13, 660. doi:10.3390/atmos13050660
- Tao, S., and Wei, J. (2006). The westward, northward advance of the subtropical high over the west pacific in summer. *J. Appl. Meteor.* 17, 513–525. doi:10.3969/j.issn.1001-7313.2006.05.001
- Wang, T., Yang, S., Wen, Z., Wu, R., and Zhao, P. (2011). Variations of the winter India-Burma Trough and their links to climate anomalies over southern and eastern Asia. *J. Geophys. Res. Atmos.* 116. doi:10.1029/2011jd016373
- Wang, Y., Peng, Z., Wu, H., and Wang, P. (2022). Spatiotemporal variability in precipitation extremes in the Jianghuai region of China and the analysis of its circulation features. *Sustainability* 14, 6680. doi:10.3390/su14116680
- Wen, M., He, J. H., and Tan, Y. K. (2003). MoveMent of the ridge line of summer west pacific subtropical high and its possible mechanism. *J. Acta Meteorol. Sin.* 17, 37–51.
- Wu, R., and Chen, S. (2020). What leads to persisting surface air temperature anomalies from winter to following spring over mid- to high-latitude Eurasia? *J. Clim.* 33, 5861–5883. doi:10.1175/jcli-d-19-0819.1
- Wu, S., and Guo, D. (2019). Effects of East Asian summer monsoon and western pacific subtropical high on summer precipitation in China. *Sci. Technol. Innov. Her.* 16, 112–119. doi:10.16660/j.cnki.1674-098X.2019.16.112
- Yang, C., Yu, Z., Hao, Z., Zhang, J., and Zhu, J. (2012). Impact of climate change on flood and drought events in Huaihe River Basin, China. *J. Hydrology Res.* 43, 14–22. doi:10.2166/nh.2011.112
- Yang, H., and Sun, S. Q. (2003). Longitudinal displacement of the subtropical high in the western Pacific in summer and its influence. *J. Adv. Atmos. Sci.* 20, 921–933. doi:10.1007/bf02915515
- Yang, K., Cai, W., Huang, G., Hu, K., Ng, B., and Wang, G. (2022a). Increased variability of the western Pacific subtropical high under greenhouse warming. *Proc. Natl. Acad. Sci.* 119, 23. doi:10.1073/pnas.2120335119
- Yang, R., Xie, Z., and Cao, J. (2017). A dynamic index for the westward ridge point variability of the western pacific subtropical high during summer. *J. Clim.* 30, 3325–3341. doi:10.1175/jcli-d-16-0434.1
- Yang, Y., Liu, C., Ou, N., Liao, X., Cao, N., Chen, N., et al. (2022b). Moisture transport and contribution to the continental precipitation. *Atmosphere* 13, 1694. doi:10.3390/atmos13101694
- Yu, S., Shi, X., and Lin, X. (2009). Interannual variation of East Asian summer monsoon and its impacts on general circulation and precipitation. *J. Geogr. Sci.* 19, 67–80. doi:10.1007/s11442-009-0067-3
- Zhang, F., Yang, X., Sun, Q., Yao, S., and Guo, Q. (2022). Three-dimensional structural anomalies of the western pacific subtropical high ridge and its relationship with precipitation in China during august–september 2021. *Atmosphere* 13, 1089. doi:10.3390/atmos13071089
- Zhang, Q., Zheng, Y., Singh, V. P., Luo, M., and Xie, Z. (2017). Summer extreme precipitation in eastern China: mechanisms and impacts. *J. Geophys. Res. Atmos.* 122, 2766–2778. doi:10.1002/2016jd025913
- Zhou, T. J., and Yu, R. C. (2005). Atmospheric water vapor transport associated with typical anomalous summer rainfall patterns in China. *J. Geophys. Res.* 110, D08104. doi:10.1029/2004JD005413
- Zhu, Y., Wang, H., Zhou, W., and Ma, J. (2011). Recent changes in the summer precipitation pattern in East China and the background circulation. *Clim. Dyn.* 36, 1463–1473. doi:10.1007/s00382-010-0852-9